Materials Characterization 121 (2016) 135–138

Contents lists available at ScienceDirect

Materials Characterization

journal homepage: www.elsevier.com/locate/matchar

Deformation induced dynamic recrystallization and precipitation strengthening in an Mg—Zn—Mn alloy processed by high strain rate rolling

Jimiao Jiang [a], Min Song [a], Hongge Yan [b], Chao Yang [a], Song Ni [a,*]

[a] State Key Laboratory of Powder Metallurgy, Central South University, Changsha 410083, China
[b] School of Materials Science and Engineering, Hunan University, Changsha 410082, China

ARTICLE INFO

Article history:
Received 2 August 2016
Received in revised form 21 September 2016
Accepted 21 September 2016
Available online 21 September 2016

Keywords:
Mg—Zn alloy
Dynamic recrystallization
Dynamic precipitation
High strain rates rolling

ABSTRACT

The microstructure of a high strain-rate rolled Mg—Zn—Mn alloy was investigated by transmission electron microscopy to understand the relationship between the microstructure and mechanical properties. The results indicate that: (1) a bimodal microstructure consisting of the fine dynamic recrystallized grains and the largely deformed grains was formed; (2) a large number of dynamic precipitates including plate-like $MgZn_2$ phase, spherical $MgZn_2$ phase and spherical Mn particles distribute uniformly in the grains; (3) the major facets of many plate-like $MgZn_2$ precipitates deviated several to tens of degrees (3°–30°) from the matrix basal plane. It has been shown that the high strength of the alloy is attributed to the formation of the bimodal microstructure, dynamic precipitation, and the interaction between the dislocations and the dynamic precipitates.

1. Introduction

Magnesium (Mg) alloys have great potential as structural materials because they are the lightest materials in structural applications. Since the stacking fault energy (SFE) of Mg is smaller than that of most light metals, such as aluminum (Al) [1], grain refinement by dynamic recrystallization (DRX) occurs quite readily. Hot deformation accompanied by DRX is a promising method for refining the microstructure and attaining superior properties of Mg alloys, such as high strength [2–4], toughness [5] and ductility [6]. On the other hand, precipitation strengthening [7] is another effective method to significantly improve the strength due to the pinning effect of precipitates on dislocation movements. Precipitates can always be obtained by artificial aging [8,9]. Mg—Zn-based alloys were among the firstly developed precipitation hardenable Mg alloys, and the strengthening precipitates include rod-like β'_1 phase (distributed along $[0001]_\alpha$ direction) with a monoclinic structure similar to Mg_4Zn_7, and plate-like β'_2 phase (also distributed along $[0001]_\alpha$ direction) with a hexagonal structure of $MgZn_2$. Recent investigations [10,11] showed that dynamic precipitates formed during hot deformation have excellent hardening effect in Mg—Al alloy. For example, Mg—8Al alloy sheet rolled at 748 K [10] has a yield strength (YS) of 321 MPa and ultimate tensile strength (UTS) of 424 MPa due to the dynamic precipitation strengthening by $Mg_{17}Al_{12}$. Mg—Al—Ca—Mn alloy fabricated by extrusion [11] has a YS and an UTS of 410 MPa and 420 MPa, respectively, due to the formation of plate-like Al—Ca precipitates and spherical Al—Mn—Ca precipitates. In our previous investigation, an Mg—Zn—Mn alloy with excellent mechanical properties (359 MPa in UTS, 258 MPa in YS, and 20.1% in elongation) was fabricated successfully by high strain-rate rolling (HSRR) at 300 °C [12]. These mechanical property values are much higher than those of most Mg—Zn—Mn alloys processed by other fabrication methods [13–16]. It is believed that grain refinement through DRX and dynamic precipitates formed during HSRR are the two main reasons accounting for the enhanced mechanical properties. In this paper, the microstructures for DRX and dynamic precipitation were thoroughly investigated via transmission electron microscopy (TEM) to understand the exact reason for the excellent mechanical properties of the alloy.

2. Experimental Detail

The ZM51 (Mg—5%Zn—1%Mn, in wt.%) alloy billets were prepared by permanent mould casting and were then annealed by two-step homogenization treatment (330 °C for 24 h and 400 °C for 2 h). Before hot rolling, the homogenization treated plates were preheated at 300 °C for 6 min. Then the plates were hot rolled with a reduction of 80% in thickness from 10 mm to 2 mm by a single pass at 300 °C with a strain rate ($\dot{\bar{\varepsilon}}$) of 9.1 s^{-1}. The microstructures of the rolled sheets were investigated by a JEOL-2100F TEM and a Titan G2 60-300 TEM. TEM samples were prepared by cutting the slices (2 mm in thickness)

* Corresponding author.
E-mail address: song.ni@csu.edu.cn (S. Ni).

http://dx.doi.org/10.1016/j.matchar.2016.09.025
1044-5803/

from the ingot using a low-speed diamond saw, then mechanical thinning the slices by sand paper to 60 μm in thickness and ion thinning using a Gatan Precision Ion Polishing System at 2 kV.

3. Results and Discussion

Fig. 1a shows a typical TEM image of the specimen after HSRR. It can be seen that a lot of dynamic recrystallized (DRXed) grains formed during HSRR with a grain size of about 0.5–2 μm. Fig. 1b shows another TEM image of the specimen, indicating that in addition to the DRXed grains in area I, largely deformed grains with size of several to tens of micrometers were observed, as shown in area II. Statistical analysis on TEM images indicate that the areas with the fine DRXed grains take up 92% of the total area of the specimen, while the rest are the largely deformed grains, forming a bimodal microstructure. The dislocation density in the deformed grains is visibly higher than that in the DRXed grains from Fig. 1b. In area II, the orientation of numerous micro-bands and slip bands is parallel to the basal plane, as shown by the red line in Fig. 1b. At the same time, several micro-bands orientated along the pyramidal plane, as shown by the green line, can be observed in areas B and C (depicted by green ellipses). Area A (depicted by yellow ellipse) is a transition zone for the micro-bands orientated along the basal plane to the pyramidal plane. The ladder-like slip lines in area A may be attributed to the cross-slip from the basal plane to the pyramidal plane.

Fig. 2a is a TEM image showing the microstructure of cross-slip in a largely deformed grain. The corresponding selected area electron diffraction (SAED) pattern was inserted at the left upper corner. No diffraction spot for twins can be observed. The cross-slip lines with abundant zigzag slip bands, which have not been observed in the as-homogenized material [12], have been produced in the process of HSRR. The details of the rectangle area in Fig. 2a are shown in Fig. 2b. Slip bands along basal plane were indicated by red solid lines, while the slip bands along the pyramidal plane that deviate a large angle from the basal plane were marked by green dashed lines. It is obvious in Fig. 2b that there are more basal slip lines than pyramidal slip lines and lots of jogs were formed (depicted by ellipse) when the basal slip lines meet the pyramidal slip lines.

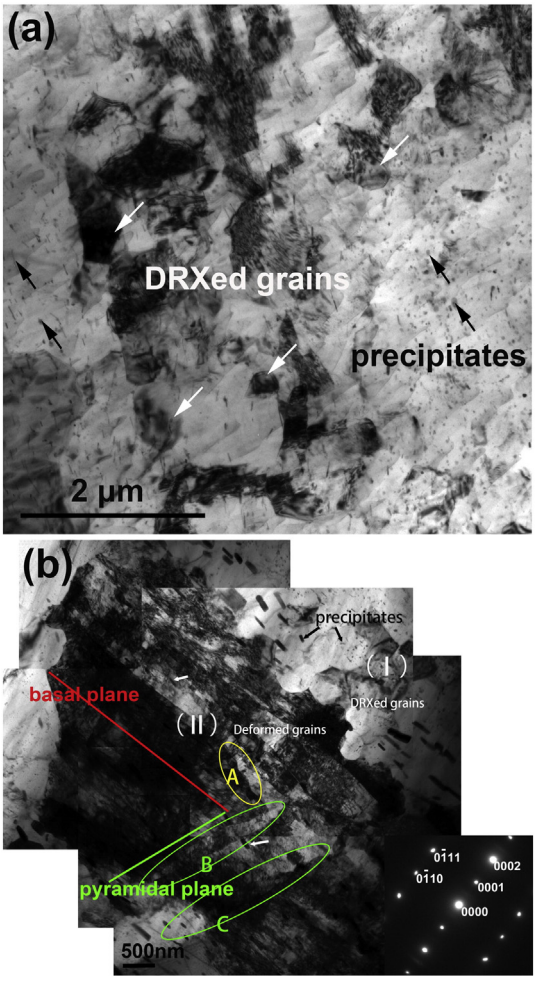

Fig. 1. Bright field TEM images of (a) the DRXed grains and (b) the largely deformed grains.

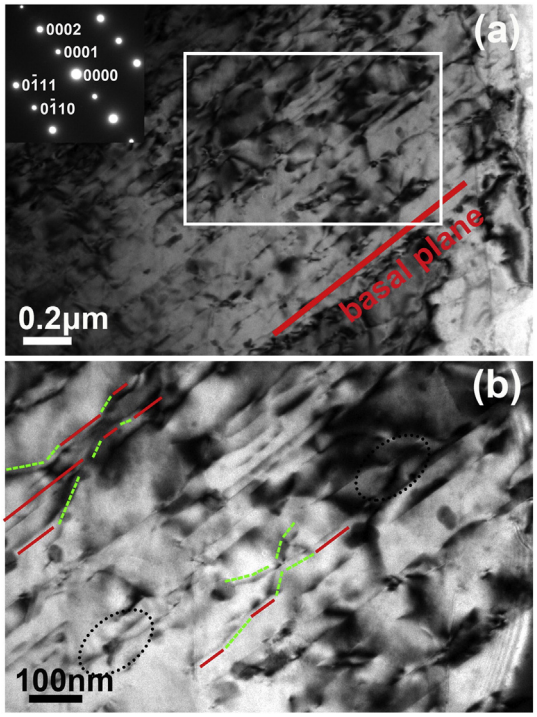

Fig. 2. (a) Bright field TEM image of the largely deformed grains and (b) the magnified image of the framed region in (a).

Fig. 3 shows the distribution of the precipitates in the alloy after HSRR along the matrix $[11\text{-}20]_\alpha$ zone axis (Fig. 3a) and $[0001]_\alpha$ zone axis (Fig. 3b), respectively. A large number of the precipitates distribute uniformly in the grain. Compared to the as-homogenized alloy in our previous investigation [12], the number of the precipitates increases sharply after HSRR. There are two types of precipitates according to their shape when observing along the matrix $[11\text{-}20]_\alpha$ zone axis: parallelogram with the length of 50–250 nm (indicated by arrow 1 in Fig. 3a) and ellipse with the size of 5–50 nm (indicated by arrows 2, 3 in Fig. 3a). However, only one type of the precipitates can be observed along the matrix $[0001]_\alpha$ zone axis: spherical or ellipse shape, with the radium ranging from 5 nm to 150 nm, as indicated by arrows 1, 2, 3 in Fig. 3b. The precipitates can thus be divided into two types based on their shape: One is the plate precipitate with the habit plane along the basal plane or pyramidal plane, and the other is the sphere precipitate.

Further investigation shows that the plate and sphere precipitates can be further divided into four kinds. Fig. 3c and d show a plate precipitate and its corresponding SAED pattern. The SEAD pattern can be indexed into $MgZn_2$ phase. The orientation relationship implied by the SAED pattern is $[10\text{-}10]_\beta \parallel [11\text{-}20]_\alpha$, $(0002)_\beta \parallel (0001)_\alpha$ and $(11\text{-}22)_\beta \parallel (10\text{-}11)_\alpha$. It can be seen from Fig. 3c that the major facets (broad surface) of the plate are the basal plane of Mg matrix. Fig. 3e shows another plate precipitate, which can also be indexed into $MgZn_2$ phase from the corresponding SEAD pattern (Fig. 3f). While the orientation relationship of the plate is $[11\text{-}20]_\beta \parallel [2\text{-}311]_\alpha$, $(0\text{-}1\text{-}1\text{-}3)_\beta \parallel (0002)_\alpha$ and $(10\text{-}1\text{-}2)_\beta \parallel (0\text{-}111)_\alpha$, differing from that of the former $(0001)_\alpha$ plate. From the TEM image and calculation, the major facets of this plate deviate 11.4° from